

**SPECIAL FEATURE:  
COMMENTARY**

# Some tenets pertaining to electrospray ionization mass spectrometry

**Richard B. Cole\***

Department of Chemistry, University of New Orleans, New Orleans, Louisiana 70148, USA

The field of electrospray ionization mass spectrometry is reviewed with emphasis placed upon advances in the elucidation of fundamental mechanistic aspects of the ionization process that have been reported over the past 10 years. The analytical consequences of these findings are also examined. Eight central conclusions or 'tenets' are presented, as deduced from the body of work contained in 80 references. Copyright © 2000 John Wiley & Sons, Ltd.

KEYWORDS: electrospray; ionization; mechanism; fundamentals; review

## INTRODUCTION

In recollecting the day that Graham Cooks approached me about writing an article describing 'What we know for sure about electrospray,' my immediate reaction was to perceive the proposition as a challenge. Was it the appropriate time? Had the field matured sufficiently beyond the clamorous debates of the mid-1990s? Could the cacophony of the annual 'showdowns' at ASMS meetings and workshops where view and rebuttal, point and counterpoint had raged for years, now be restructured into a harmonious symphony? I thought back to a conversation that I had in 1995 with John Fenn where he had aptly analogized the state of the debate on the mechanism of electrospray ionization at that time to the classic children's story of the Blind Men and the Elephant. As you will recall, each man described the elephant in a completely different manner, depending on the body part that he was touching. I asked myself 'are we still blind men?' Could one possibly write a consensus article if no consensus existed? I confirmed my willingness to participate in the project and stumbled off to search for some aspirin.

The structure of this presentation represents something of a departure in form from those of previous reviews of electrospray phenomena. This commentary is organized in the framework of a few brief statements (herein referred to as 'tenets') regarding mechanistic and analytical aspects of electrospray that have been elucidated owing to the considerable efforts and creativity of many individuals working in the field. Particular effort has been made to highlight advances that were achieved within the decade of the 1990s. Owing to space limitations and the desire

to cover a wide range of sub-topics, it was not possible to discuss every nuance of each issue. Furthermore, the list of eight tenets is by no means exhaustive, nor is it intended to represent a final version or definitive depiction of the electrospray process. Rather, it is a compilation of a limited number of conclusions, supported by experimental evidence, that were not obvious a decade ago when the greying cloud of potential electrospray applications looming overhead was just about to burst open. Of course, in hindsight, the keys that one had struggled to find to unlock a mystery, often dangle so blatantly in view. Finally, if this list may inspire the elucidation of some yet undiscovered 'tenets of the future,' I look forward to it becoming less and less complete as time rolls on.

## 1. THE ELECTROSPRAY ION SOURCE HAS OPERATIONAL CHARACTERISTICS OF A CONTROLLED-CURRENT ELECTROLYTIC FLOW CELL

In electrospray ionization (ESI), a high voltage is applied to the metal ESI capillary through which a sample solution is emerging. If the counter-electrode is large and planar compared with the working electrode, the value of the electric field,  $E_c$ , in the air at the capillary tip can be approximated from the following equation:<sup>1–3</sup>

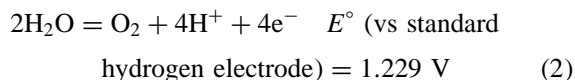
$$E_c = 2V_c/[r_c \ln(4d/r_c)] \quad (1)$$

where  $r_c$  is the capillary outer radius,  $V_c$  is the applied electric potential and  $d$  is the distance from the capillary tip to the counter-electrode. The electric field strength is typically  $\sim 10^6$ – $10^7$  V m<sup>-1</sup>.<sup>2,3</sup> As ionic species in the sample solution emerge from the ESI capillary, they undergo electrophoretic movement in response to the imposed electric field. In the positive ion mode, anions

\* Correspondence to: R. B. Cole, Department of Chemistry, University of New Orleans, New Orleans, Louisiana 70148, USA.

Contract/grant sponsor: National Science Foundation; Contract/grant number: CHE-9981948.

migrate in the direction of the metal ESI capillary (relatively positive potential), whereas cations migrate away from the metal capillary in the direction of the counter-electrode. The electric field that gives a push to the positive ions is counterbalanced by the surface tension of the liquid. At sufficiently high electric field strengths a dynamic cone of liquid referred to as a 'Taylor cone'<sup>4</sup> will form at the capillary exit. Owing to the high voltage difference between the ESI capillary and the counter-electrode, oxidation reactions occur at the metal–solution interface of the ESI capillary. These oxidation processes (positive ion mode) may take several forms, such as H<sup>+</sup> production from water:<sup>5–7</sup>



In the negative ion mode, of course, the direction of electrophoretic movement of anions and cations is reversed relative to the above discussion, and reduction reactions occur at the metal ESI capillary. These electrochemical reactions are essential to sustaining the continuous production of charged droplets of one polarity. Similarly, at the counter-electrode where there is a continuous arrival of charged species of one polarity, it is necessary to perform a second electrochemical reaction. In the positive ion mode, this second reaction must be a reduction. Logically, the counter-electrode reaction in the negative ion mode is an oxidation. When this second reaction occurs, a special type of electrical circuit has been completed. Accordingly, Kebarle and co-workers<sup>3,8</sup> recognized the electrospray source as a special type of electrolytic cell in which electrolysis maintains the charge balance to allow continuous production of charged droplets.

Further refinement of the description of the electrolytic nature of the electrospray source by Van Berkel and Zhou<sup>6,9</sup> led to its characterization as a controlled-current electrolytic (CCE) flow cell. Thus, the potential at the solution–ESI capillary interface is a function of the magnitude of the ESI current, and the redox potentials and concentrations of solution species. In positive ion experiments, the implication is that in order to supply a certain demanded ESI current, the potential at the electrode/solution interface attains a value to permit the oxidation process that is characterized by the lowest oxidation potential, as determined by the solution components and the materials present in the capillary (Fig. 1). If the conversion rate of the most electroactive species at the metal–solution interface is insufficient to produce the required current, the potential will rise to a point where the next most easily oxidized species undergoes electron removal, and so on, until the demanded current is produced.<sup>6,9</sup>

The current,  $i_{\text{ES}}$ , at the electrospray capillary (equivalent to the rate at which charge leaves the capillary in the form of charged droplets) has been expressed in the theoretically derived Hendricks equation,<sup>2</sup> presented here in modified<sup>5,9</sup> form:

$$i_{\text{ES}} = H v_f^\nu \sigma_s^n E_c^\varepsilon \quad (3)$$

where  $H$  is a constant whose value will vary depending upon the dielectric constant and the surface tension of the

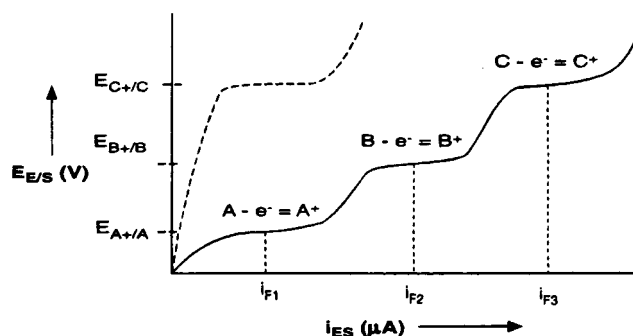


**Figure 1.** Schematic illustration showing the expected interdependence of the potential at the electrode–solution interface,  $E_{E/S}$ , in the ES capillary as a function of the ES current,  $i_{\text{ES}}$ , based on the operation of an ES ion source as a controlled-current electrolytic cell. Solid line: three electroactive species, A, B and C, are present in the solution at equal concentration, with electrode potentials  $E_{A+/A} < E_{B+/B} < E_{C+/C}$ . Dashed line: only the electroactive species C is contained in the solution. Reprinted with permission of the American Chemical Society from Ref. 9.

solvent,  $v_f$  is the flow-rate,  $\sigma_s$  is the specific conductivity and  $E_c$  is the imposed electric field [see Eqn (1)]. Some work has been performed to experimentally evaluate the exponents  $\nu$ ,  $n$ , and  $\varepsilon$ , and the values obtained (all  $>0$ ) were found to correlate reasonably well with those predicted by the Hendricks equation.<sup>5,10</sup> G. J. Van Berkel (unpublished results) observed that the actual values of the exponents were interdependent, with the product of the three exponents ( $\nu n \varepsilon$ ) giving an approximately constant value of about 4/7. Employing 1-octanol solutions containing volume fractions of H<sub>2</sub>SO<sub>4</sub> varying from 0.3 to 0.5%, Fernandez de la Mora and Loscertales<sup>11</sup> reported that the current varies in proportion to the square root of flow-rate and electrical conductivity (i.e.  $\nu = 1/2$  and  $n = 1/2$ ).

Evidence to support the analogy to the CCE flow cell came from experiments wherein  $i_{\text{ES}}$  was raised by augmenting solution conductivity (as predicted by the Hendricks equation) and the amount of electroactive analyte (porphyrin) undergoing oxidation was observed to increase.<sup>6,9</sup> In the absence of electrolyte, very low currents were anticipated and observed. In this case, oxidation of the porphyrin did not occur, presumably because sufficient quantities of more easily oxidized contaminants were present to maintain the lower current levels, hence the value of the interfacial potential within the capillary,  $E_{E/S}$ , was below the minimum required to oxidize the analyte. However, when the magnitude of  $i_{\text{ES}}$  was increased, either by elevating the electrolyte concentration (and thus conductivity) or by raising  $E_c$ , porphyrin oxidation was observed. Further corroboration of the CCE nature of the ESI source came when a more easily oxidized electrolyte (ferrocene) was added to porphyrin solutions causing oxidation of the latter to be shut down, while addition of anthracene (more difficult to oxidize) resulted in no oxidation of anthracene.<sup>6,9</sup>

Although electrolytic processes are often transparent to the end user (particularly in cases where electrolysis products are non-ionic or have low desorption coefficients), it should be noted that when aqueous solutions are employed, pH changes attributable to the electrochemical reaction of water can affect the appearance of the mass spectrum. The effect will be particularly pronounced when

low flow-rates such as those common to the nanospray mode (tens of  $\text{nl min}^{-1}$ ) are employed, non-buffered solutions are used and/or difficult to oxidize metals constitute the spray capillary (or contacts).<sup>7</sup> In these cases, the availability of protons relative to other cations in the final droplets is likely to have been altered significantly during the ESI process. Such a change can substantially influence the abundances of protonated and multiply protonated molecules versus other types of solution cations, and it will also exert a more subtle effect on the charge state distributions of multiply protonated species. These latter two factors may have important consequences for quantitative analyses.<sup>7</sup>

## 2. DROPLET-JET FISSION INCREMENTALLY BOOSTS THE CHARGE-TO-MASS RATIO IN 'OFFSPRING' DROPLETS

At the origin of the continuous production of charged species of a given polarity are electrochemical redox processes that occur at the ESI capillary. The excess charges accumulate near the end of the capillary and are electrically attracted to the counter-electrode, causing the emerging liquid to elongate in the direction of the counter-electrode. It is the surface tension of the liquid, however, that provides an opposing force to hold the solution together. The balancing of these two opposing forces results in the formation of the dynamic Taylor cone<sup>4</sup> at the exit of the ESI capillary. At the apex of the Taylor cone a 'jet' of liquid emerges wherein the charge density attains such a high value that the surface tension can no longer hold together the emerging fluid. As charged droplets emanate from the tip of the jet, stability has been gained by droplet breakup because the excess charges are spread over a larger surface area, thereby reducing the Coulomb energy. This process produces a fine spray of charged droplets of a single polarity that are directed toward the counter-electrode owing to the potential and, to a lesser extent, pressure gradients.

The radius of the jet emerging from the Taylor cone, and hence, the initial radii of the formed droplets increase approximately in proportion to  $(\text{flow-rate})^{2/3}$ , as given by Fernandez de la Mora *et al.*<sup>12</sup> The radius of generated charged droplets will also increase with decreasing conductivity. This implies that the use of high conductivity solutions and low flow-rates will result in the production of the smallest droplets. The integrated charge emerging from the ESI capillary in pulsed fashion (i.e. in the form of charged droplets) can be considered as the 'ESI current,' and its magnitude is equal to the current generated by electrochemical reactions at the capillary tip if 'corona' discharges are not occurring. Electrical (corona) discharges can also contribute to current at the ESI capillary, but via a gas-discharge mechanism that the experimentalist usually tries to minimize.<sup>13–15</sup> The ESI current provides a quantitative estimate of the maximum number of available charges that can be converted into gas-phase ions,<sup>16,17</sup> and substantial fluctuations in the current are indicators of spray instability and/or electrical discharge.

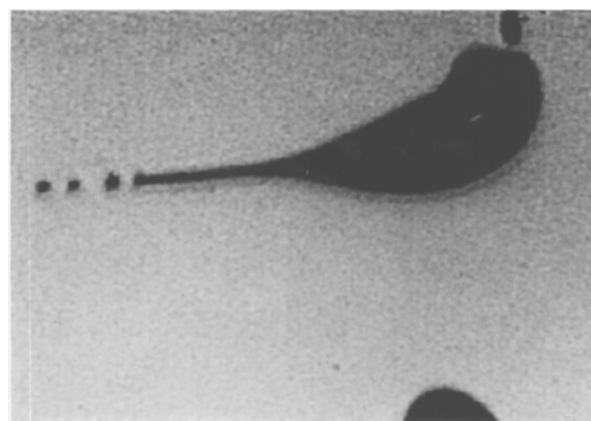
As the solvent evaporates from charged droplets, usually with assistance from resistive heating, the size of

the droplets becomes smaller, but the charge that they carry remains constant. This results in increasing electrostatic stress near the surface of a given droplet. When the force of electrostatic repulsion between like charges becomes equal to the surface tension force holding the droplet together, the so-called 'Rayleigh stability limit' has been reached as defined by the Rayleigh equation:<sup>3,18</sup>

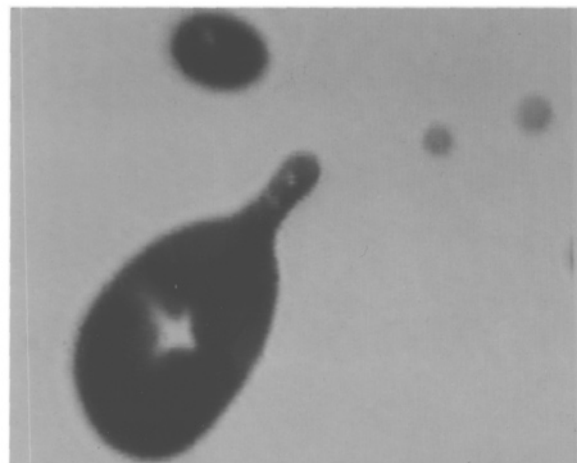
$$q_R = 8\pi(\epsilon_0\gamma R^3)^{1/2} \quad (4)$$

where  $q$  is the excess charge on the droplet of radius  $R$ ,  $\gamma$  is the surface tension and  $\epsilon_0$  is the permittivity of vacuum.

Just prior to reaching the Rayleigh stability limit, droplets undergo what is referred to as 'Coulomb fission,' a process which leads to the production of smaller 'offspring' droplets. Thus, charged droplets are not static entities, but rather they may distort from spherical into oblate or prolate shapes.<sup>5,19</sup> Shape irregularities of this type stimulate disruptions in which a 'stream' of much smaller droplets are emitted in what was originally termed an 'uneven fission' event because the combined total of offspring droplets carry off only about 1–2.3% of the mass and 10–18% of the charge of the parent droplet.<sup>20</sup> Figure 2 (from Gomez and Tang<sup>19</sup>) shows a photograph of an uneven fission event, more recently referred to as 'droplet-jet fission,'<sup>3</sup> in progress. A monodisperse distribution of



(a)



(b)

**Figure 2.** Flash shadowgraphs showing droplets undergoing Coulomb fission. The mean flow direction is from top to bottom. Reprinted with permission of American Institute of Physics from Ref. 19.

offspring droplet sizes having radii roughly one-tenth that of the parent droplets is obtained. The charge-to-mass ratio is thus increased in the offspring droplets relative to the parent droplet which produced them, but the overall repulsive force of like charges near the droplet surfaces is attenuated because the charge is spread over a larger total surface area. The droplet-jet fission process may repeat itself a second, and perhaps a third, time upon further shrinkage of the offspring droplets.

---

### 3. ANALYTE CHARGING AND DESORPTION ARE DRIVEN BY EXCESS CHARGES PRESENT IN FINAL DROPLETS

---

Since the inception of electrospray ionization,<sup>21,22</sup> the concept of droplet fission, be it in unrefined form, was linked to the formation of gas-phase ions. However, in the early 1990s, many different views existed concerning the relationship between the degree of charge associated with an ion in a neutral solution (as determined by solution-phase equilibria) and the distribution of charge states observed in the ESI mass spectrum.<sup>23–26</sup> Early reports on the multiple charging phenomenon correlated the number of basic sites on protein molecules to the number of charges (protons) that could attach and were retained on analyte molecules in obtained ESI mass spectra.<sup>27–30</sup>

An apparent contradiction was posed by the observations of Fenselau and co-workers,<sup>24</sup> where, in the positive mode, an envelope of ions corresponding to multiply protonated myoglobin with a maximum charge state of +14 was obtained from initially basic solutions (pH 10). At this basic pH, solution-phase protonation is known to be minimal, and myoglobin exists virtually exclusively in anionic form. Moreover, in the negative ion mode employing initial solutions of pH 3, an envelope of multiply deprotonated myoglobin molecules was observed to have a maximum charge state of –11, even though it is well known that myoglobin exists virtually completely in cationic form in solutions of this acidity.

Two explanations have been put forth to rationalize the observation of these so-called ‘wrong-way-round’ ions. Le Blanc *et al.*<sup>26</sup> proposed that when small nitrogen bases (e.g. amines) have been added to solution, multiply protonated proteins desorb with the nitrogen bases attached. The desorbed complexes may then dissociate in the gas phase, resulting in the partitioning of available charge (protons) between the polypeptide and the nitrogen base. More recently, Boyd and co-workers<sup>31</sup> have rationalized the appearance of protonated molecules (MH<sup>+</sup>) in ESI mass spectra obtained from strongly basic solutions where initial solution protonation of analyte molecules was negligible. An electrolyte which cannot be considered to be a source of protons (i.e. tetramethylammonium hydroxide) was used to raise the solution pH. A mechanism was proposed entailing formation of a complex involving the analyte molecule, a tetramethylammonium cation and water (solvent). The cation was proposed to induce dissociation of water thus forming a [cation + hydroxide] ion pair, with concomitant release of a proton. This liberated proton originating from the solvent attaches to the analyte molecule as desolvation reaches completion, thus forming a gas-phase protonated molecule.

This scenario involving indirect liberation of protons originating from the solvent can explain the origin of multiply protonated molecules that arise from highly basic solutions, where initial solution protonation is negligible. The existence of these ‘wrong-way-round’ ions serves as evidence that it is the charge imbalance in the final droplets that drives analyte charging and desorption. While neutral solution equilibria certainly determine the initial ionic character of the analyte, it is the excess charges in the final droplets that ultimately impart charge (be it directly or indirectly) to the gas-phase ions.

Definitive proof that droplet charging and solvent evaporation will lead to the release of gas-phase ions even in the absence of a Taylor cone was provided by so-called ‘droplet electrospray’ experiments<sup>32</sup> wherein charge was imparted to neutral falling droplets via a gas discharge process. In this arrangement, non-analyte ions formed during the gas discharge enter the initially neutral droplets, thus creating charged droplets in an alternative fashion to the solution electrochemistry process outlined above in Tenet 1. It was found that sample solutions that were charged in this manner gave mass spectra virtually identical with those of the same solutions run by conventional ESI-MS. This observation implies that the cations originating from the gas discharge process were converted to ion-paired species within the droplets, thus liberating positive charges which ultimately served to charge the analyte in the gas phase after droplet-jet fission occurred.

---

### 4. LARGE MOLECULES ARE IONIZED ACCORDING TO A CHARGED RESIDUE SCENARIO

---

Two principal mechanisms have been put forward to explain the process by which gas-phase ions originate from small, highly charged droplets. The first mechanism, initially proposed by Dole and co-workers,<sup>21,22</sup> depicts a series of fission events that ultimately leads to the production of final small droplets that bear one or more excess charges, but only a single analyte molecule. As the last few solvent molecules evaporate, the excess charges present will become situated on the sites affording the most stable gas-phase analyte ion. This scenario is referred to as the *charged residue model* (CRM). Dole and co-workers reasoned that if the original concentration was sufficiently low, repeated Coulomb fission would produce droplets that contained only a single analyte molecule. This analyte molecule would retain the ‘residual’ droplet charge as the last solvent molecules evaporated, thus forming a ‘free’ gas-phase ion.

The second mechanism, proposed by Iribarne and Thomson,<sup>33,34</sup> contends that solvated ions are emitted directly from charged droplets after the radii of the droplets decrease to a suitable size. This depiction is termed the *ion evaporation mechanism* (IEM). Iribarne and Thomson reasoned that at a certain point prior to the Rayleigh limit (e.g. radius <10 nm), the electric field on the surface of the charged droplets is sufficiently high that solvated ions may be emitted into the gas phase. They proposed that at an intermediate stage of the charged

droplet's lifetime, the charge density on the droplet surface, while still less than the Rayleigh limit, was sufficiently high to lift a charged analyte molecule, entraining with it a few solvent molecules, from the droplet surface into the ambient gas.

A fundamental distinction between the CRM and the IEM lies in the manner whereby an analyte molecule becomes separated from other solute molecules contained in the droplet.<sup>35</sup> In the IEM, separation occurs when a single solvated analyte ion carrying some of the droplet's charge is desorbed into the gas phase, thereby attenuating Coulomb repulsion. In the CRM, separation occurs via successive fission events that ultimately produce final charged droplets that contain only one analyte molecule. However, this distinction can become foggy if one attempts to differentiate between the desorption of a single solvated ion from a parent droplet (IEM) and a final Coulomb fission event that produces an ultimate droplet consisting of a single analyte molecule in the presence of excess charges and a few solvent molecules (CRM). Moreover, any differences in the number of charges or the degree of solvation found in a desorbed ion produced by an IEM scenario versus those found in an ultimate charged droplet produced by CRM are not likely to be pronounced.

Despite the above controversy, a solid consensus has emerged that ionic forms of very large molecules, including multiply charged varieties, are formed in ESI-MS according to a charged residue mechanism.<sup>35–39</sup> Fenn *et al.*<sup>35</sup> cite the CRM as being applicable when the solute molecule has linear dimensions significantly larger than the charged droplet that contains it. Most recently, Fernandez de la Mora<sup>37</sup> gave evidence that the maximum charge on several globular proteins retaining a compact structure, and several compact 'starburst' dendrimers, was between 65 and 110% of the charge corresponding to the Rayleigh limit calculated for these spherical structures (as shown in Fig. 3). Because the charge carried by the compact polymers constitutes such a large proportion of the maximum allowable charge given by the Rayleigh limit, it was concluded that a charged residue scenario was at work for molecules having masses above at least 3300 Da. It was further rationalized that after the last fission event leading

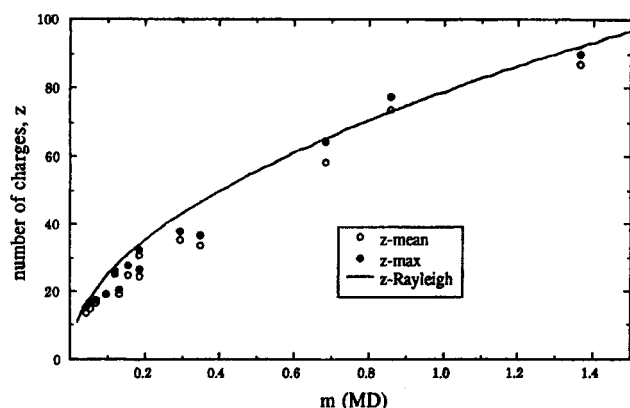


**Figure 3.** Maximum and mean charge on various native proteins compared with the Rayleigh limit (continuous curve). Molecular weights of the proteins given on the x-axis are in units of  $10^6$  Da. Data points are taken from Tolic *et al.*<sup>80</sup> Reprinted from *Analytica Chimica Acta*, **406**, J. Fernandez de la Mora, "Electrospray ionization species proceeds via Dole's charged residue mechanism", p. 97, © 2000 Elsevier Science Ltd.

up to formation of the spherical residue, this residue contains, on average, about 70% of the charge corresponding to the Rayleigh limit. Upon departure of the last solvent molecules, these charges (whose number relates to the Rayleigh limit) become attached to the gas-phase dendrimers. On the other hand, if these compact polymer ions were desorbed by an ion evaporation scenario, the charge of a dendrimer ion would be governed by the evaporation dynamics of this large polymer, and would not be expected to correlate to the anticipated Rayleigh limit.<sup>37</sup>

The debate still rages over the mechanism of desorption of smaller ions. The latest jousting has taken place in the domain of the salt clusters. Employing a differential mobility analyzer and a particle size magnifier, Gamero-Castano and Fernandez de la Mora<sup>40</sup> put forward the view that ion evaporation is responsible for the production of tetraheptylammonium bromide clusters observed to contain as many as 18 ion pairs. They used highly conductive solutions to suppress Coulomb fissions (instead charge is shed by ion evaporation), thereby inhibiting tetraheptylammonium bromide cluster ion formation via a charged residue mechanism. Employing alkali metal halides as test compounds, Kebarle and Peschke<sup>38</sup> come down on the same side of the fence as the above authors, pointing especially to the higher abundances of  $\text{Na}^+$  relative to  $\text{Na}(\text{NaCl})_n^+$  that are predicted by IEM. Their experimentally determined monatomic ion:cluster ion ratios were found to correspond more closely to IEM predictions than CRM predictions, although the predicted abundances of the  $\text{Na}(\text{NaCl})_n^+$  clusters were somewhat lower than the observed values.

In rebuttal and championing the opposing view, Wang and Cole<sup>39,41</sup> argue that because a series of triatomic alkali metal halide ions with well-defined properties, and characterized by higher solvation enthalpies, are observed in consistently higher abundances than those of an analogous series characterized by lower solvation enthalpies, a charged residue scenario is responsible for the formation of these triatomic (and larger) clusters. They argue that an ion evaporation mechanism would predict the opposite trend. The teams of Kebarle and Peschke<sup>38</sup> and Wang and Cole<sup>39,41</sup> both acknowledge certain unproven assumptions made in asserting their respective viewpoints. Moreover, both research teams report their respective estimates of the most probable *dominant* mechanism, without excluding the other mechanism as a less favored pathway.

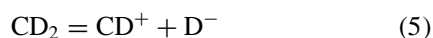
## 5. HIGHER POLARITY SOLVENTS LEAD TO HIGHER CHARGE STATES OF MULTIPLY CHARGED IONS

The ability to form ions characterized by very high charge states is unique, among mass spectrometric ionization methods, to electrospray ionization. Multiply charged ions observed in ESI-MS arise from molecules that have undergone multiple protonations or attachment of several cations (positive ion mode), or have undergone removal of multiple protons or attachment of several anions (negative ion mode). A typical mass spectrum of a 'pure' compound thereby contains a series of peaks that are all

representative of intact molecules that differ in the number of charges that they carry. The appearance of the mass spectral 'envelope' (i.e. range of charge states observed, most abundant charge state, relative abundances of ions) depends upon a combination of analyte, solution, gas-phase and instrumental factors.<sup>42</sup>

The characteristics of the solvent influence the formation of gas-phase ions in a multitude of ways. For example, the onset potential for electrospray (i.e. the minimum voltage required to form the Taylor cone<sup>4</sup>) increases with solution surface tension, the spray current increases with solution conductivity, and the initial droplet size increases with solvent viscosity.<sup>43</sup> A higher solvent polarity shifts dissociation equilibria to favor the formation of higher charge state ions in solution. In turn, the appearance of more highly charged ions has been observed in the gas phase.

As examples of simple analytes that have the possibility to undergo multiple charging, diquatery ammonium salts represented as  $CD_2$ , where  $C^{2+}$  is the diquatery ammonium dication and  $D^-$  is the counterion (e.g.,  $Cl^-$ ,  $CF_3COO^-$ ), were examined in the positive ion mode:<sup>44</sup>



Each of the above dissociation equilibria shifts to the right in solvents of higher polarity. It should be noted that the use of these diquatery ammonium salts avoids any question of association/dissociation equilibria involving protons because the 'permanent' charges remain fixed on the two nitrogen atoms. As illustrated in Fig. 4, raising the solvent polarity (upward movement in Fig. 4) was shown to shift consistently the charge states of these diquatery ammonium salts towards the 2+ state in ESI mass spectra. Analogous results were obtained in the negative ion mode.<sup>45</sup>

These findings indicate that solvents of higher polarity (as measured, for example, by the dielectric constant) can offer improved stabilization to charge separation in solution. This can, in turn, facilitate the process of 'electrophoretic' charging wherein solution anions migrate towards the positively charged ESI capillary (positive ion mode). The greater degree of charge separation and the higher stability afforded to ions via solvation by higher polarity solvents leads to a shift in charge states towards higher values in the ESI mass spectrum. Although the fate of the original counterions is not known for certain, higher polarity solvents may (1) facilitate their removal at the ESI capillary via electrochemical processes, (2) impede the transfer of counterions to offspring droplets during droplet-jet fission events and/or (3) decrease the tendency for counterions to remain attached to multiply charged analyte ions desorbing into the gas phase.

It should be noted parenthetically that solvent polarity can also exert a profound influence on the predominant form of analyte anions appearing in negative ion ESI mass spectra. When a competition was set up between deprotonation (to form  $[M - H]^-$ ) and anion attachment (to form  $[M + Cl]^-$ ), higher polarity solvents consistently favored the formation of  $[M - H]^-$ .<sup>46</sup> Once again, it seems logical that the improved charge separation afforded by solvents of higher polarity stabilizes charge separation of the analyte molecule; in this case charge separation involves dissociation of a proton.

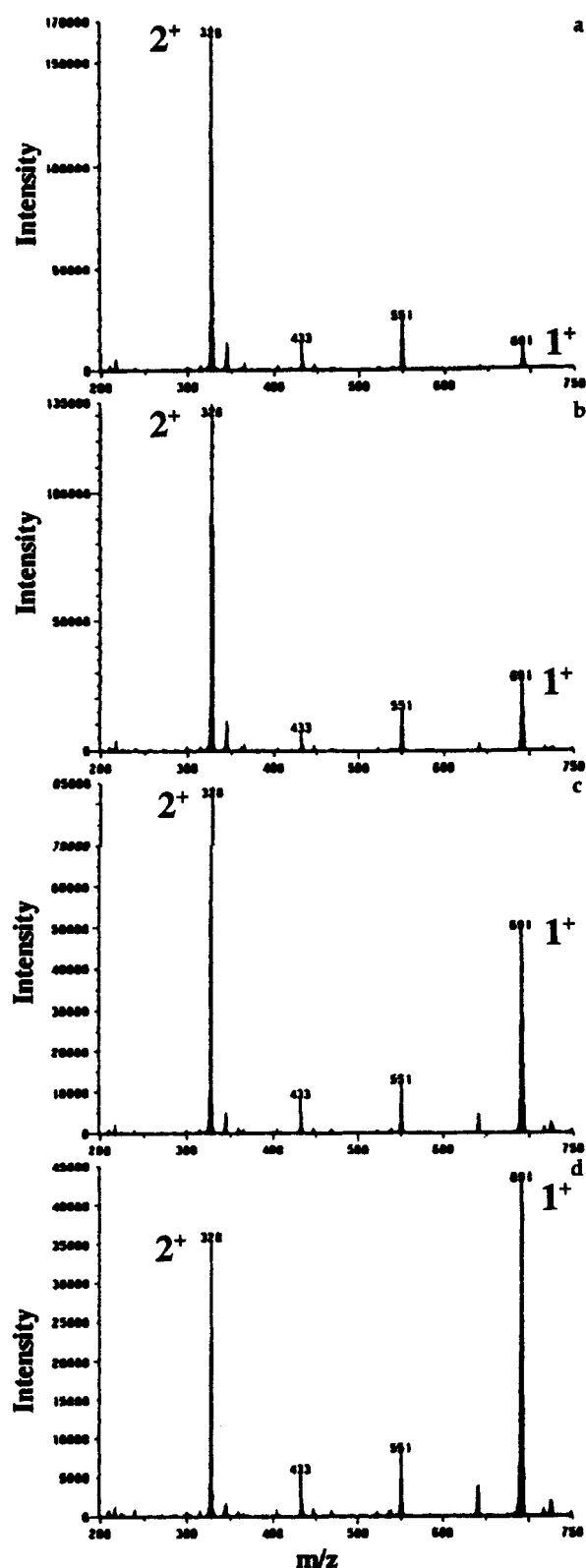


**Figure 4.** Electrospray ionization mass spectra of a  $5 \times 10^{-5}$  M diquatery ammonium chloride salt in alcohol solvents arranged in order of decreasing polarity: (a) methanol; (b) ethanol; (c) 1-propanol; and (d) 1-butanol. The peaks at  $m/z$  691 and 328 represent  $[M - Cl]^+$  and  $[M - 2Cl]^{2+}$ , respectively. Reprinted from the Journal of the American Society for Mass Spectrometry, 7, G. Wang and R. B. Cole, "Effects of solvent and counterion on ion pairing and observed charge states of diquatery ammonium salts in electrospray ionization mass spectrometry", p. 1052, © 1999, with permission from Elsevier Science Ltd.

## 6. GAS-PHASE PROCESSES INTIMATELY INFLUENCE THE MAXIMUM CHARGE STATE, CHARGE STATE DISTRIBUTION AND SIGNAL INTENSITY

As the final solvent molecules depart from a solvated ion that has been desorbed by either ion evaporation or by a charged residue scenario, one may consider the interactions between the remaining few molecules and charges to be true gas-phase interactions. Williams and co-workers<sup>47–50</sup> considered that the most acidic proton on a multiply protonated peptide,<sup>47</sup> protein<sup>47,48</sup> or diaminoalkane<sup>49</sup> cluster containing one or more solvent molecules would be attracted by the solvating influence of electrons located on the most basic unoccupied site of the multiply charged molecule, as well as by those of the last few solvent molecules. They postulated that a certain 'pull' was exerted on the proton by the multiply protonated molecule, the magnitude of which was determined by the latter's 'apparent gas-phase basicity',<sup>47,48</sup> i.e., the intrinsic gas-phase basicity of the remaining unprotonated site characterized by the highest basicity, minus the coulomb energy exerted by existing charges upon this site. An opposing 'pull' was exerted by the remaining solvent whose magnitude was determined by the gas-phase basicity of the solvent molecule(s). They reasoned that the maximum charge state obtainable for a given multiply charged ion was determined in this final competition between the highly charged ion and the solvent. When the multiply charged ion bore so many protons (occupying the sites of highest basicity) such that the next proton to be added could not be afforded the stability that it would enjoy attached to a single solvent molecule, the point of maximum analyte charge state had been reached.

Figure 5 illustrates the decrease in apparent gas-phase basicity as the charge state of a protein (cytochrome *c*)

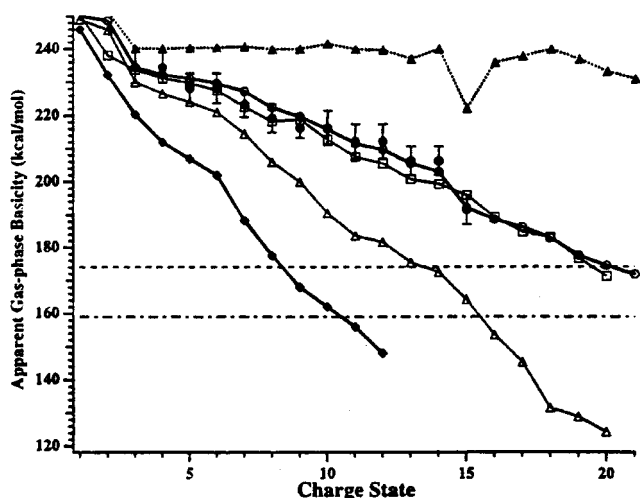


**Figure 5.** Apparent gas-phase basicity as a function of charge state of cytochrome *c* ions: measured (solid circles); calculated, linear (open circles); intrinsic (solid triangles); calculated, x-ray crystal structure (solid diamonds); calculated,  $\alpha$ -helix (open squares). The dashed line denotes the gas-phase basicity of methanol [ $174.1 \text{ kcal mol}^{-1}$  ( $1 \text{ kcal} = 4.184 \text{ kJ}$ )] and the dashed dotted line indicates the gas-phase basicity of water ( $159.0 \text{ kcal mol}^{-1}$ ). Reprinted with permission of the American Chemical Society from Ref. 48.

is increased.<sup>48</sup> Horizontal lines indicate the gas-phase basicities of methanol and water solvents. Protein charge states corresponding to points below the horizontal line of the solvent are not expected to appear in the ESI mass spectrum. Apparent gas-phase basicities calculated by Williams and co-workers<sup>47</sup> led to predictions of maximum charge states that correlated well with experimental values found in the literature, pointing to the conclusion that the maximum obtainable charge state for proteins is dictated by gas-phase proton transfer reactivity with residual solvent.

As mentioned under the heading Tenet 3 above, referring to solutions to which small nitrogen bases had been added, Le Blanc *et al.*<sup>26</sup> proposed that gas-phase dissociations of protonated nitrogen bases could occur from desorbed complexes consisting of multiply protonated proteins bearing nitrogen bases held on by electrostatic attraction of the nitrogen lone pair. The subsequent departures of protonated nitrogen bases were then cited as the underlying cause for a shift in analyte protein charge states to lower values. This type of dissociation that can radically alter observed charge state distributions was proposed to occur in the gas phase.

More recent examples of the influence upon the ESI mass spectrum of residual solvent molecules still clinging to gas-phase analyte ions are elaborated upon in Enke and co-workers<sup>51</sup> feature article in this issue detailing positive ion mode experiments, and in negative ion work involving chloride anion attachment to neutral molecules contained in a variety of chlorinated solvents.<sup>52</sup> In comparing solvents of differing chloride affinities and employing aniline as an analyte that produces no  $[\text{M} - \text{H}]^-$  signal, it was established that chloroform solvent (relatively high chloride affinity) scavenged most available chloride anions, leaving almost none to attach to neutral aniline molecules, thus yielding a very weak  $[\text{aniline} + \text{Cl}]^-$  signal in the shadow of a towering  $[\text{chloroform} + \text{Cl}]^-$  peak. However, when carbon tetrachloride (very low chloride affinity) was employed as the solvent, a strong signal for  $[\text{aniline} + \text{Cl}]^-$  appeared as the base peak with no detectable  $[\text{CCl}_4 + \text{Cl}]^-$  peak. Interestingly, owing to the presence of chloroform as a trace impurity in the reagent-grade carbon tetrachloride, a sizeable  $[\text{CHCl}_3 + \text{Cl}]^-$  peak was present.<sup>52</sup> The presence of this peak reinforces the notion that gas-phase 'tugs-of-war' to capture the  $\text{Cl}^-$  anions occur among the final few droplet constituents. While carbon tetrachloride obviously cannot compete, aniline was present in overwhelming concentration relative to chloroform in this latter system, but the superior strength of chloroform binding apparently became highly determinant as fewer and fewer other molecules remained.

## 7. HIGHEST ABSOLUTE SENSITIVITY IS OBTAINED FROM SINGLE-ANALYTE SOLUTIONS RUN AT THE LOWEST FLOW-RATE THROUGH NARROW DIAMETER CAPILLARIES

The types of molecules that can be detected via ESI-MS range from organic or inorganic salts that are inherently charged in solution, to polar neutral species that exhibit association/dissociation dynamics of small ions such as

protons, to non-polar species that undergo electrochemical oxidation/reduction at the ESI capillary.<sup>53–55</sup> The biggest restriction is that analytes must dissolve in a solvent exhibiting moderate conductivity.<sup>43,56,57</sup> Notably, analytes exhibiting a higher degree of surface activity are known to produce higher intensity signals up to a certain size limit. The increased response is attributed to improved desorption characteristics of the surface-active compounds.<sup>35,36,58</sup>

The solution containing even a purified analyte that is to undergo ESI analysis cannot be considered to be a 'single electrolyte' system. Electrochemical reaction products are present (see Tenet 1), and impurities may inevitably enter from various sources, including reagent-grade solvents that often contain  $\sim 10^{-5}$  M  $\text{Na}^+$ , or contamination of the capillary line and fittings. Moreover, electrolytes are often added to sample solutions to promote desorption of specific types of ions (e.g. acid, to promote the formation of  $\text{MH}^+$ , or base, to increase the yield of  $[\text{M} - \text{H}]^-$ ). The presence of high quantities of added electrolytes will result in the suppression of analyte signals.<sup>58,59</sup> The magnitude of the suppression will depend upon the relative desorption characteristics of the analyte (that are highly influenced by properties such as surface activity) versus those of the other electrolytes present. In practical terms, analyte signal suppression caused by competing electrolytes (including other analytes) is one of the major shortcomings of electrospray ionization mass spectrometry, and solutions containing high-concentration electrolytes should be avoided. Signal suppression may prevent the successful analyses of complex mixtures, especially when only trace quantities of the compound(s) of interest are present. In these cases, chromatographic isolation (either off-line or on-line) of the target compounds prior to ESI-MS analysis can result in vastly improved signals.

To handle high solution flow-rates [e.g.  $20 \mu\text{l min}^{-1}$  to  $2 \text{ ml min}^{-1}$  used in conventional liquid chromatography (LC)], many ESI sources incorporate a counterflow stream of bath gas,<sup>60</sup> pneumatically assisted nebulization,<sup>61,62</sup> and/or heating<sup>63,64</sup> to facilitate liquid break-up. In a device providing pneumatic assistance, high-pressure nitrogen delivered to the region where solution is emerging from the ESI capillary provides a shearing force to aid aerosol formation, as both gas and liquid are forced out of a small orifice. It is important to note, however, that the best sensitivities are usually obtained in the absence of a nebulizer gas. Ultrasonic nebulizers<sup>62</sup> can also assist liquid break-up at higher flow-rates. For sample solutions of high aqueous content, such as mobile phases commonly employed in reversed-phase LC, pneumatically-assisted nebulizers and ultrasonic nebulizers can be particularly useful. Of course, both approaches still rely on an imposed electric field to induce droplet charging.

When conventional  $\mu\text{l min}^{-1}$  flow-rates are employed, ESI is characterized as a 'concentration-sensitive' technique, meaning that signal strength is proportional to concentration. This implies that in this regime, neither subtle changes in flow-rate nor flow splitting (e.g. of post-column LC effluent) will significantly alter sensitivity. On the other hand, at the extremely low flow-rates of the so-called 'nanoflow' regime (i.e.  $\sim 10\text{--}100 \text{ nl min}^{-1}$ ), the ionization efficiency can approach 100%. Here, ESI is

described as 'mass flux sensitive' (i.e. response is proportional to the absolute quantity or 'mass' of material present).<sup>65</sup>

The number of charges per droplet and the radius of the initial droplet are both dependent on the solution flow-rate. Wilm and Mann<sup>66,67</sup> reasoned that in the nanoflow regime, smaller droplets characterized by higher surface-to-volume ratios permit higher desorption efficiencies of charged analyte molecules. In addition, the smaller aperture capillaries (i.e.  $1\text{--}2 \mu\text{m}$  inner diameter) employed give a narrower dispersion of sprayed droplets, hence sample transfer into the mass spectrometer is more efficient. A  $\sim 20 \text{ nl min}^{-1}$  flow-rate may thus increase overall ionization efficiency by more than two orders of magnitude<sup>67</sup> compared with the conventional  $\mu\text{l min}^{-1}$  range. Nanoflow sprayers yield droplets sizes below 200 nm.<sup>66,67</sup> The improved ionization efficiency and high ion desorption rates have resulted in reports of extremely low limits of detection, such as  $5 \text{ amol ml}^{-1}$  (i.e.  $5 \times 10^{-18} \text{ mol ml}^{-1}$ ) for methionine-enkephalin,<sup>68</sup> and  $32 \text{ amol ml}^{-1}$  for neurotensin.<sup>69</sup> Furthermore, low flow-rates clearly allow for reduced sample consumption and extended acquisition times, a combination that can lead to improved signal-to-noise ratios via signal averaging over extended time periods.

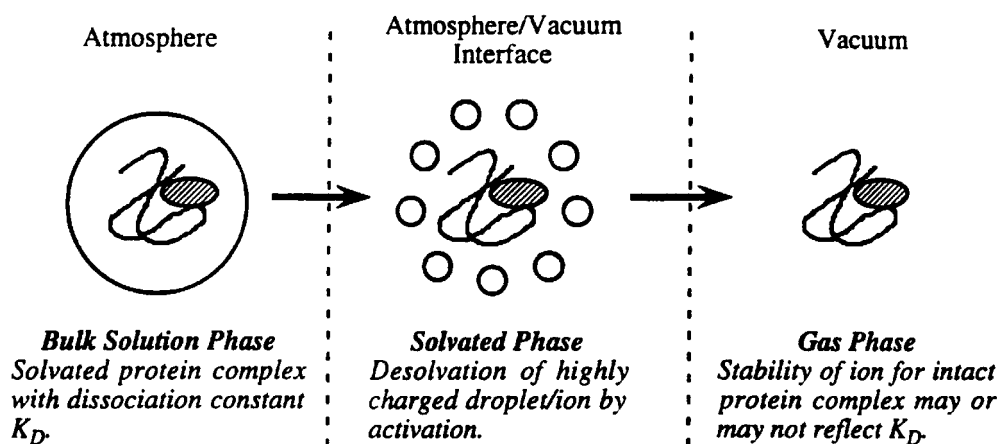
---

## 8. THE AMOUNT OF INTERNAL ENERGY IMPARTED TO GENERATED IONS IS THE LOWEST OF ALL MASS SPECTROMETRIC IONIZATION TECHNIQUES

---

Compared with other desorption/ionization methods, evidence suggests that electrospray is a 'softer' ionization method. Wysocki and co-workers<sup>70</sup> showed that  $\text{MH}^+$  ions desorbed by ESI are cooler than the same protonated molecules produced by liquid secondary ion mass spectrometry (LSIMS). In the same vein, the distribution of  $\text{MH}^+$  ion structures was not as complex as that obtained by LSIMS, and a stable form was shown to dominate in ESI for small peptides containing a basic amino acid. In the ESI process, it seems reasonable that the internal energy (vibrational and rotational) of a charged analyte-solvent cluster is dissipated during the desolvation stage when loosely bound solvent molecules dissociate from the final charged analyte ion. An outcome is that an extremely low degree of fragmentation is inherent to the electrospray ionization process.

If more structural information is desired from an ESI mass spectrum without performing a true MS/MS experiment, fragmentation can be promoted by varying the potential difference between the 'cone' and the 'skimmer' (effectively changing the velocity of the ions that have exited the cone).<sup>42</sup> The pressure in the region between cone and skimmer [typically  $\sim 10^{-2}$  Torr ( $1 \text{ Torr} = 133.3 \text{ Pa}$ )] is low enough to allow an ion a significant mean free path of travel before collision occurs, yet high enough that the probability for collision is still significant. Energetic collisions between ions and residual gas molecules will thus result. Such collision-induced dissociation (CID) processes, referred to as 'in-source CID' or 'nozzle-skimmer CID,' will serve to break apart residual cluster ions, even at extremely

**ESI-MS of Noncovalently Bound Protein Complexes**

**Figure 6.** Schematic depiction of solvent evaporation and the transfer of a non-covalently bound complex from solution to the gas phase. Gentle desolvation conditions favor the detection of the intact gas-phase complex. Several protein systems yield ESI-MS data that are consistent with the solution-phase binding constants. However, the stability of the gas-phase complex ion is not necessarily reflected by the solution-phase binding constant. Reprinted with permission of John Wiley & Sons, Inc. from Ref. 78.

low energies. At higher energies, fragmentation of analyte ions will occur. Because the velocity of ions in the region just after the cone is determined in large part by the voltage drop between the cone and the ensuing skimmer, raising the cone voltage will provoke higher energy collisions between ions and the neutral gas molecules present, thereby inducing a higher degree of decomposition.

Obtained charge state distributions in ESI-MS will also be affected, because ions of higher charge state arising from a given molecule will undergo greater acceleration than their lower charge state counterparts (it is also likely that desolvation of higher charge state ions occurs at a slower rate). Because the number of reactive charge sites is increased, the coulomb energy is higher, and the reactivity is increased. The combination of these factors boosts the tendency for higher charge state ions to shed charges (via transfer to residual solvent, other components present in the original solution, or residual gases). The outcome is that an elevated cone voltage leads to a shift in charge state towards lower values in the ESI mass spectrum.<sup>42</sup>

Collette and De Pauw<sup>71</sup> used a 'survival yield' method to estimate the internal energy distribution of ions produced by electrospray. Experimental parameters and differences in source design<sup>72</sup> were shown to exert a substantial influence on obtained distributions. Increasing the cone voltage or the mass of the employed collision gas resulted in a shift of the internal energy distributions towards higher energies, as well as a broadening of the curve. This behavior was analogized to that of a Boltzmann (thermal) distribution. Employing a cone voltage of 15 eV, the estimate of the internal energy distribution for an electrosprayed benzyropyridinium salt yielded a probability maximum at about 0.6–0.7 eV.<sup>71</sup>

An important analytical outgrowth of the gentle nature of the transfer of analytes from solution to the gas phase in ESI is that the three-dimensional structures of compounds in solution are relatively unperturbed by the phase transition. This feature permits the mass spectrometric investigation of aspects of three-dimensional structure that are

inaccessible by other MS ionization techniques. Suckau *et al.*<sup>73</sup> established the existence of at least three distinct gaseous conformations of cytochrome *c*, and also readily distinguished between disulfide cross-linked RNase A and the denatured variety by examining the propensities for molecules to undergo hydrogen–deuterium exchange in the gas phase. At about the same time, Katta and Chait<sup>74</sup> used hydrogen–deuterium exchange to probe conformational changes of ubiquitin and lysozyme in solution. In both approaches, the degree (and rate) of hydrogen–deuterium exchange is an indicator of molecular conformation and intramolecular binding.

Finally, another important consequence of the mild nature of the ESI process is that weak binding due to *specific* non-covalent interactions that exist in solution can be preserved and studied in the gas phase. After early examples established the possibilities of probing specific binding between receptor–ligand complexes<sup>75</sup> and protein–metal ion complexes,<sup>76</sup> reports of mass spectrometrically observed non-covalent binding now abound in the literature.<sup>77–79</sup> Figure 6 illustrates in cartoon form an intact protein complex emerging into the gas-phase after desorption via ESI. The ability to preserve in the gas phase non-covalent complexes that existed in solution has opened up new worlds of investigation to the mass spectrometrist, who may nevermore be regarded as the analyst with the 'sledgehammer' touch.

### Acknowledgements

The author is indebted to group members Dr Chau-Wen Chou and Mr Bertrand Salino for their suggestions for improving the manuscript, and to former group members Dr Junhua Zhu and Dr Guangdi Wang who had each contributed to previous collaborative reviews of separate aspects of electrospray. The author extends thanks to the other feature contributors Dr Christie Enke, Dr Juan Fernandez de la Mora and Dr Gary Van Berkel along with feature coordinator Dr R. Graham Cooks for their constructive criticisms of the manuscript. The author expresses the utmost gratitude to Dr Dominique Custos for *terra firma* support throughout the project. Financial support for this endeavor was provided by the National Science Foundation through grant CHE-9981948.

## REFERENCES

- Loeb LB, Kip AF, Hudson GG, Bennett WH. *Phys. Rev.* 1941; **60**: 714.
- Pfeifer RJ, Hendricks CD. *AIAA J.* 1968; **6**: 496.
- Kebarle P, Ho Y. In *Electrospray Ionization Mass Spectrometry: Fundamentals, Instrumentation and Applications*, Cole RB (ed.). John Wiley & Sons: New York, 1997; 3–63.
- Taylor GI. *Proc. R. Soc. London, Ser. A* 1964; **280**: 383.
- Kebarle P, Tang L. *Anal. Chem.* 1993; **65**: 972A.
- Van Berkel GJ. In *Electrospray Ionization Mass Spectrometry: Fundamentals, Instrumentation and Applications*, Cole RB (ed.). John Wiley & Sons: New York, 1997; 65–105.
- Van Berkel GJ, Zhou F, Aronson JT. *Int. J. Mass Spectrom. Ion Processes* 1997; **162**: 55.
- Blades AT, Ikononou MG, Kebarle P. *Anal. Chem.* 1991; **63**: 2109.
- Van Berkel GJ, Zhou F. *Anal. Chem.* 1995; **67**: 2916.
- Tang L, Kebarle P. *Anal. Chem.* 1991; **63**: 2709.
- Fernandez de la Mora J, Loscertales IG. *J. Fluid Mech.* 1994; **260**: 155.
- Fernandez de la Mora J, Navascues J, Fernandez F, Rosell-Llompart J. *J. Aerosol. Sci.* 1990; **21**: 5673.
- Ikononou MG, Blades AT, Kebarle P. *J. Am. Soc. Mass Spectrom.* 1991; **2**: 497.
- Cole RB, Harrata AK. *Rapid Commun. Mass Spectrom.* 1992; **6**: 536.
- Wampler FM, Blades AT, Kebarle P. *J. Am. Soc. Mass Spectrom.* 1993; **4**: 289.
- Wang G, Cole RB. *Anal. Chem.* 1995; **67**: 2892.
- Enke CG. *Anal. Chem.* 1997; **69**: 4885.
- Lord Rayleigh. *Philos. Mag.* 1882; **14**: 184.
- Gomez A, Tang K. *Phys. Fluids* 1994; **6**: 404.
- Taffin DC, Ward TL, Davis EJ. *Langmuir* 1989; **5**: 376.
- Dole M, Mack LL, Hines RL, Mobley RC, Ferguson LD, Alice MB. *J. Chem. Phys.* 1968; **49**: 2240.
- Mack LL, Kralik P, Rheude A, Dole M. *J. Chem. Phys.* 1970; **52**: 4977.
- Guevremont R, Siu KWM, Le Blanc JCY, Berman SS. *J. Am. Soc. Mass Spectrom.* 1992; **3**: 216.
- Kelly MA, Vestling MM, Fenselau CC, Smith PB. *Org. Mass Spectrom.* 1992; **27**: 1143.
- Wang G, Cole RB. *Org. Mass Spectrom.* 1994; **29**: 419.
- Le Blanc JCY, Wang J, Guevremont R, Siu KWM. *Org. Mass Spectrom.* 1994; **29**: 587.
- Covey TR, Bonner RF, Shushan BI, Henion J. *Rapid Commun. Mass Spectrom.* 1988; **2**: 249.
- Loo JA, Udseth HR, Smith RD. *Biomed. Environ. Mass Spectrom.* 1990; **29**: 419.
- Loo JA, Edmonds CG, Udseth HR, Smith RD. *Anal. Chem.* 1990; **62**: 693.
- Smith RD, Loo JA, Ogorzalek Loo RR, Busman M, Udseth HR. *Mass Spectrom. Rev.* 1991; **10**: 359.
- Mansoori BA, Volmer DA, Boyd RK. *Rapid Commun. Mass Spectrom.* 1997; **11**: 1120.
- Hager DB, Dovichi NJ, Klassen J, Kebarle P. *Anal. Chem.* 1994; **66**: 3944.
- Iribarne JV, Thomson BA. *J. Chem. Phys.* 1976; **64**: 2287.
- Thomson BA, Iribarne JV. *J. Chem. Phys.* 1979; **71**: 4451.
- Fenn JB, Rosell J, Nohmi T, Banks Jr FJ. In *Biochemical and Biotechnological Applications of Electrospray Ionization Mass Spectrometry*, Snyder AP (ed.). American Chemical Society: Washington, DC, 1995; 60–80.
- Fenn JB. *J. Am. Soc. Mass Spectrom.* 1993; **4**: 524.
- Fernandez de la Mora J. *Anal. Chim. Acta* 2000; **406**: 93.
- Kebarle P, Peschke M. *Anal. Chim. Acta* 2000; **406**: 11.
- Wang G, Cole RB. *Anal. Chim. Acta* 2000; **406**: 53.
- Gamero-Castano M, Fernandez de la Mora J. *Anal. Chim. Acta* 2000; **406**: 67.
- Wang G, Cole RB. *Anal. Chem.* 1998; **70**: 873.
- Wang G, Cole RB. In *Electrospray Ionization Mass Spectrometry: Fundamentals, Instrumentation and Applications*, Cole RB (ed.). John Wiley & Sons: New York, 1997; 137–174.
- Smith DPH. *IEEE Trans. Ind. Appl.* 1986; **IA-22**: 527.
- Wang G, Cole RB. *J. Am. Soc. Mass Spectrom.* 1996; **7**: 1050.
- Cole RB, Harrata AK. *J. Am. Soc. Mass Spectrom.* 1993; **4**: 546.
- Cole RB, Zhu J. *Rapid Commun. Mass Spectrom.* 1999; **13**: 607.
- Schnier PD, Gross DS, Williams ER. *J. Am. Soc. Mass Spectrom.* 1995; **6**: 1086.
- Schnier PD, Gross DS, Williams ER. *J. Am. Chem. Soc.* 1995; **117**: 6747.
- Gross DS, Rodriguez-Cruz SE, Bock S, Williams ER. *J. Phys. Chem.* 1995; **99**: 4034.
- Williams ER. *J. Mass Spectrom.* 1996; **31**: 831.
- Amad MH, Cech NB, Jackson GS, Enke CG. *J. Mass Spectrom.* 2000; **35**: 784.
- Zhu J, Cole RB. *J. Am. Soc. Mass Spectrom.* in press.
- Van Berkel GJ, McLuckey SA, Glish GL. *Anal. Chem.* 1992; **64**: 1586.
- Anacleto JF, Quilliam MA, Boyd RK, Howard JB, Lafleur AL, Yadav T. *Rapid Commun. Mass Spectrom.* 1993; **7**: 229.
- Xu X, Nolan SP, Cole RB. *Anal. Chem.* 1994; **66**: 119.
- Hayati I, Bailey AI, Tadros ThF. *Nature, (London)* 1986; **319**: 41.
- Hayati I, Bailey AI, Tadros ThF. *J. Colloid Interface Sci.* 1987; **117**: 205.
- Tang L, Kebarle P. *Anal. Chem.* 1993; **65**: 3654.
- Tang L, Kebarle P. *Anal. Chem.* 1991; **63**: 2709.
- Whitehouse CM, Dreyer RN, Yamashita M, Fenn JB. *Anal. Chem.* 1985; **57**: 675.
- Bruins AP, Covey TR, Henion JD. *Anal. Chem.* 1987; **59**: 2642.
- Bruins AP. In *Electrospray Ionization Mass Spectrometry: Fundamentals, Instrumentation and Applications*, Cole RB (ed.). John Wiley & Sons: New York, 1997; 107–136.
- Chowdhury SK, Katta V, Chait BT. *Rapid Commun. Mass Spectrom.* 1990; **4**: 81.
- Ikononou MG, Kebarle P. *J. Am. Soc. Mass Spectrom.* 1994; **5**: 791.
- Covey T. In *Biochemical and Biotechnological Applications of Electrospray Ionization Mass Spectrometry*, Snyder AP (ed.). American Chemical Society: Washington, DC, 1995; 21–59.
- Wilm M, Mann M. *Int. J. Mass Spectrom. Ion Processes* 1994; **136**: 167.
- Wilm M, Mann M. *Anal. Chem.* 1996; **68**: 1.
- Emmett MR, Caprioli RM. *J. Am. Soc. Mass Spectrom.* 1994; **5**: 605.
- Andren PE, Emmett MR, Caprioli RM. *J. Am. Soc. Mass Spectrom.* 1994; **5**: 867.
- Jones JL, Dongre AR, Somogyi A, Wysocki VH. *J. Am. Chem. Soc.* 1994; **116**: 8368.
- Collette C, De Pauw E. *Rapid Commun. Mass Spectrom.* 1998; **12**: 165.
- Collette C, Drahos L, De Pauw E, Vekey K. *Rapid Commun. Mass Spectrom.* 1998; **12**: 1673.
- Suckau D, Shi Y, Beu SC, Senko MW, Quinn JP, Wampler FW, McLafferty FW. *Proc. Natl. Acad. Sci. USA* 1993; **90**: 790.
- Katta V, Chait BT. *J. Am. Chem. Soc.* 1993; **115**: 6317.
- Ganem B, Li Y-T, Henion JD. *J. Am. Chem. Soc.* 1991; **113**: 6294.
- Katta V, Chait BT. *J. Am. Chem. Soc.* 1991; **113**: 8534.
- Loo JA. *Mass Spectrom. Rev.* 1997; **16**: 1.
- Loo JA, Loo RRO. In *Electrospray Ionization Mass Spectrometry: Fundamentals, Instrumentation and Applications*, Cole RB (ed.). John Wiley & Sons: New York, 1997; 385–419.
- Pramanik BN, Bartner PL, Mirza UA, Liu Y-H, Ganguly AK. *J. Mass Spectrom.* 1998; **33**: 911.
- Tolic LP, Anderson GA, Smith RD, Brothers HM, Spindler R, Tomalia DA. *Int. J. Mass Spectrom. Ion Processes* 1997; **165**: 405.